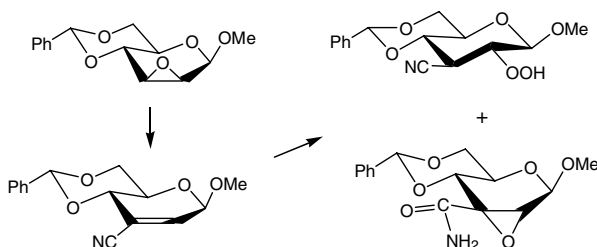


Contents

FULL PAPERS

Preparation of 2-C- and 3-C-cyano-2-enopyranoside derivatives and their epoxidation pp 2339–2353

Tohru Sakakibara,* Shinya Narumi, Ichiro Matsuo, Saeko Okada and Takanori Nakamura



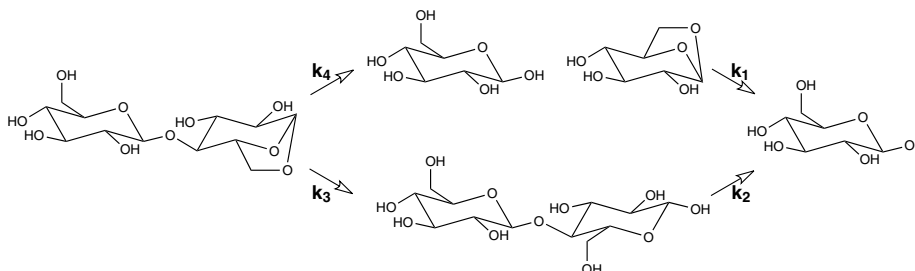
An X-ray diffraction analysis of crystallised whey and whey-permeate powders pp 2354–2364

Justin Nijdam,* Alexander Ibach, Klaus Eichhorn and Matthias Kind

Amorphous whey powders have been crystallised at various air temperatures and humidities, and these crystallised powders have been examined using X-ray diffraction. The ultimate aim of this work is to develop an industrial crystallisation process that produces stable non-caking whey powders.

A kinetic model for production of glucose by hydrolysis of levoglucosan and cellobiosan from pyrolysis oil pp 2365–2370

Steve Helle,* Nicole M. Bennett, Karen Lau, Justin H. Matsui and Sheldon J. B. Duff

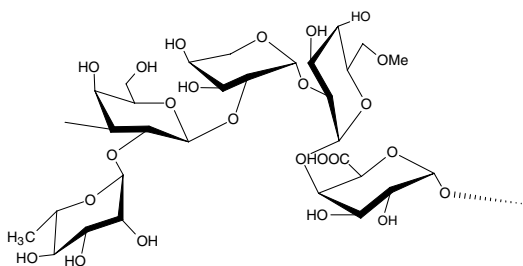


Relationship between structure and immunostimulating activity of enzymatically synthesized glycogen pp 2371–2379
 Ryo Kakutani,* Yoshiyuki Adachi, Hideki Kajiura, Hiroki Takata, Takashi Kuriki and Naohito Ohno

We established the fact that the molecular weight (5000–6500K) of glycogen is closely related to macrophage stimulation and augments the production of NO, TNF- α , and IL-6. The fine structure of the glycogen has a minor correlation with macrophage stimulation. Some experimental results indicate that the macrophage-stimulating mechanism of glycogen differs from that of LPS.

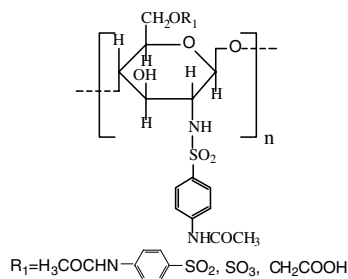
Structural investigation of a heteropolysaccharide isolated from the pods (fruits) of *Moringa oleifera* pp 2380–2389
 (Sajina)

Sadhan K. Roy, Krishnendu Chandra, Kaushik Ghosh, Subhas Mondal, Debabrata Maiti, Arnab K. Ojha, Debsankar Das, Soumitra Mondal, Indranil Chakraborty and Syed S. Islam*



Synthesis and antifungal properties of sulfanilamide derivatives of chitosan pp 2390–2395

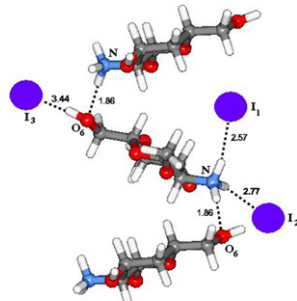
Zhimei Zhong, Rong Chen, Rong Xing, Xiaolin Chen, Song Liu, Zhanyong Guo, Xia Ji, Lin Wang and Pengcheng Li*



Six new sulfanilamide derivatives of chitosan were synthesized and their antifungal activities were reported.

Theoretical investigation of hydrogen bonding effects on oxygen, nitrogen, and hydrogen chemical shielding and electric field gradient tensors of chitosan/HI salt pp 2396–2403

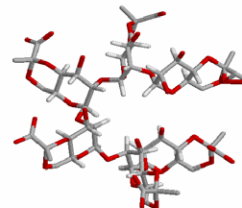
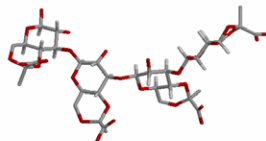
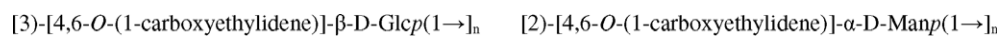
Sajjad Khodaei, Nasser L. Hadipour* and Mohammad Reza Kasaii



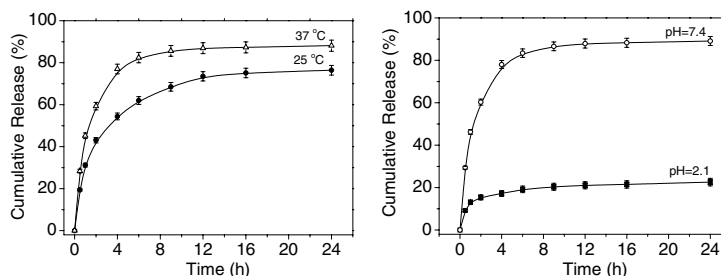
Crystalline Structure of Chitosan/HI Salt

Exopolysaccharides produced by *Inquilingus limosus*, a new pathogen of cystic fibrosis patients: novel structures with usual components pp 2404–2415

Yury Herasimenka, Paola Cescutti,* Giuseppe Impallomeni and Roberto Rizzo


Preparation and properties of a pH/temperature-responsive carboxymethyl chitosan/poly(*N*-isopropylacrylamide)semi-IPN hydrogel for oral delivery of drugs pp 2416–2422

Bao-Lin Guo and Qing-Yu Gao*



Effect of temperature and pH on release of CoA of semi-IPN15 at different temperature and pH values in solution.

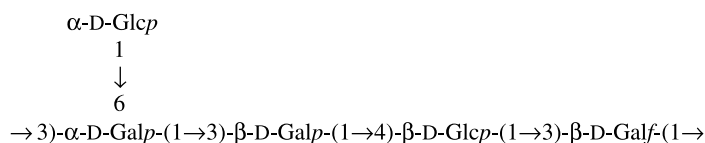
Study on the production of chitin and chitosan from shrimp shell by using *Bacillus subtilis* fermentation pp 2423–2429

Theruvathil K. Sini, Sethumadhavan Santhosh* and Paruthapara T. Mathew

Fermentation of shrimp shell in jaggery broth using *Bacillus subtilis* for the production of chitin and chitosan was investigated. It was found that *B. subtilis* produced sufficient quantity of acid to remove the minerals from the shell and to prevent spoilage organisms. The protease enzyme in *Bacillus* species was responsible for the deprotenisation of the shell. pH, proteolytic activity, extent of demineralization and deprotenisation were studied during fermentation. About 84% protein and 72% minerals were removed from shrimp shell after fermentation. Mild acid and alkali treatments were given to produce characteristic chitin and their concentrations were standardized. Chitin was converted to chitosan by N-deacetylation and the properties of chitin and chitosan were studied. FTIR spectral analysis of chitin and chitosan prepared were carried out and they are compared with the spectra of commercially available samples.

Structure of a neutral exopolysaccharide produced by *Lactobacillus delbrueckii* ssp. *bulgaricus* LBB.B26 pp 2430–2439

Inmaculada Sánchez-Medina, Gerrit J. Gerwig, Zoltan L. Urshev and Johannes P. Kamerling*

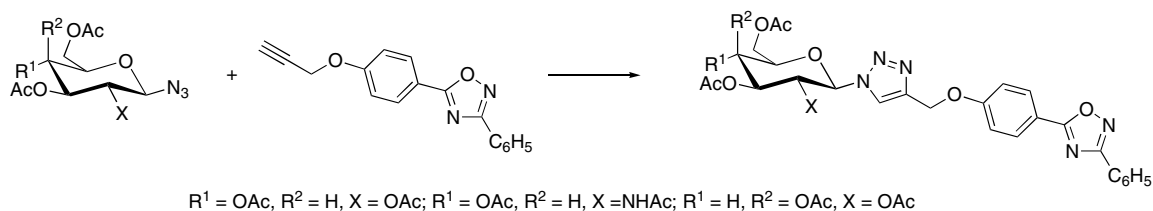


NOTES

Synthesis of glycosyl-triazole linked 1,2,4-oxadiazoles

pp 2440–2449

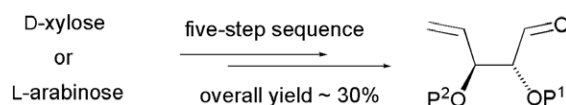
Janaina V. dos Anjos, Denis Sinou,* Sebastiao J. de Melo and Rajendra M. Srivastava*



Convenient conversion of wheat hemicelluloses pentoses (D-xylose and L-arabinose) into a common intermediate

pp 2450–2455

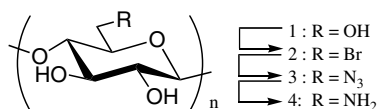
Ariane Bercier, Richard Plantier-Royon* and Charles Portella*



The application of microwave heating to the synthesis of 6-amino-6-deoxycellulose

pp 2456–2460

Toshiyuki Takano,* Junya Ishikawa, Hiroshi Kamitakahara and Fumiaki Nakatsubo

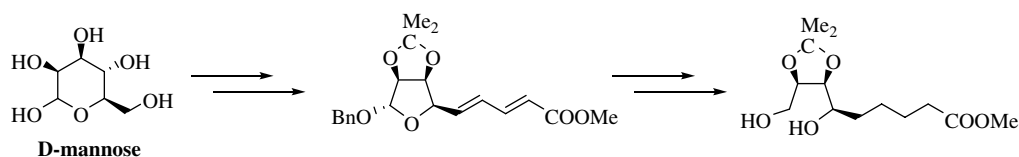


Microwave heating had the advantages of shortening reaction times and retaining of the degree of polymerization of cellulose derivatives in the synthesis of 6-amino-6-deoxycellulose.

An improved synthesis of a key intermediate for (+)-biotin from D-mannose

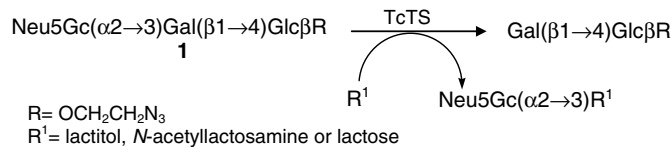
pp 2461–2464

Fen-Er Chen,* Jian-Feng Zhao, Fang-Jun Xiong, Bin Xie and Ping Zhang



The *trans*-sialidase from *Trypanosoma cruzi* efficiently transfers α -(2→3)-linked *N*-glycolylneuraminic acid to terminal β -galactosyl units pp 2465–2469

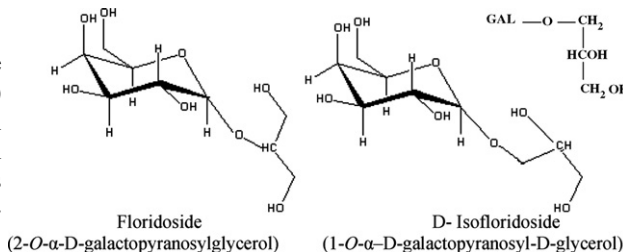
Rosalía Agustí, María Eugenia Giorgi and Rosa M. de Lederkremer*



Separation of floridoside and isofloridosides by HPLC and complete ^1H and ^{13}C NMR spectral assignments for *D*-isofloridoside pp 2470–2473

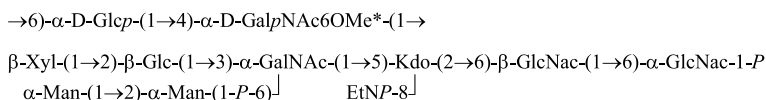
Stéphanie Bondu,* Nelly Kervarec, Eric Deslandes and Roger Pichon

This paper describes a chromatographic method for the separation of floridoside (2-*O*- α -*D*-galactopyranosylglycerol) and isofloridosides (1-*O*- α -*D*-galactopyranosyl-*D*-glycerol and 1-*O*- α -*D*-galactopyranosyl-*L*-glycerol) extracted from the red alga *Porphyra umbilicalis*. 1D/2D NMR experiments were used to fully assign the ^1H and ^{13}C spectra of *D*-isofloridoside (1-*O*- α -*D*-galactopyranosyl-*D*-glycerol).



The structure of the carbohydrate backbone of the LPS from *Myxococcus xanthus* strain DK1622 pp 2474–2480

Leann MacLean, Malcolm B. Perry, Ludmila Nossova, Heidi Kaplan and Evgeny Vinogradov*



where ac are 13-methyl-C14-3OH (*iso*-C15-3OH), C16-3OH, or 15-methyl-C16-3OH (*iso*-C17-3OH).

Characterisation of the extracellular polysaccharides produced by isolates of the fungus *Acremonium* pp 2481–2483

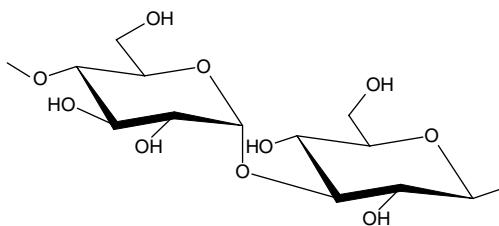
Frank Schmid, Frances Separovic, Barbara M. McDougall, Bruce A. Stone, Robert T. C. Brownlee and Robert J. Seviour*

Solid state ^{13}C NMR studies and enzymatic digestion of the extracellular glucans from the fungi *Acremonium persicinum* C38 (QM107a) and *Acremonium* sp. strain C106 indicated a backbone of (1→3)- β -linked glucosyl residues with single (1→6)- β -linked glucosyl side branches for both glucans. Average branching frequencies of these glucans were 66.7% and 28.6%, respectively.

A water-soluble glucan isolated from an edible mushroom *Termitomyces microcarpus*

pp 2484–2489

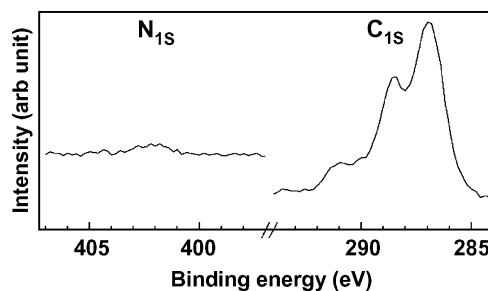
Krishnendu Chandra, Kaushik Ghosh, Sadhan K. Roy, Subhas Mondal, Debabrata Maiti, Arnab K. Ojha, Debsankar Das, Soumitra Mondal and Syed S. Islam*

**Surface structure of chitosan and hybrid chitosan-amylose films—restoration of the antibacterial properties of chitosan in the amylose film**

pp 2490–2493

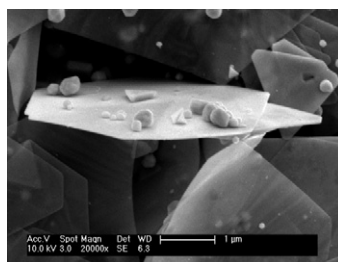
Shiho Suzuki, Bo Ying, Hideki Yamane, Hideki Tachi, Katsumasa Shimahashi, Kozo Ogawa* and Shinichi Kitamura*

The surface of an amylose–chitosan film showed clear nitrogen 1s electron in XPS. This may result in the restoration of the antibacterial property of chitosan.

**Mass synthesis of single-crystal gold nanosheets based on chitosan**

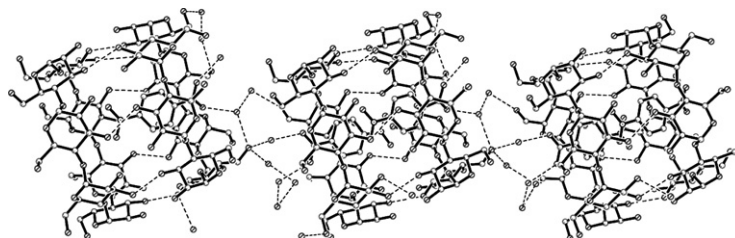
pp 2494–2499

Dongwei Wei, Weiping Qian,* Yi Shi, Shaohua Ding and Yan Xia

**An investigation of the inclusion complex of β -cyclodextrin with *p*-nitrobenzoic acid in the solid state**

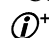
pp 2500–2503

Zhi Fan,* Chun-Hua Diao, Min-Jie Guo, Rong-Juan Du, Yuan-Fang Song, Zuo-Liang Jing and Ming Yu



The inclusion behavior of β CD with *p*-NBA shows that two β CD molecules are linked by means of hydrogen-bonds producing a barrel-like structure inside of which a pair of guest molecules is accommodated. The intervening water molecules play an important role in determining the guest position and orientation.

*Corresponding author

 Supplementary data available via ScienceDirect

COVER

The image shows the ball-and-stick representation of a potent *n*-butyl thiazoline inhibitor of *Q*-GlcNAcase, bound in the active centre of the enzyme. The work is the result of collaboration between the groups of Professors David Vocadlo (Simon Fraser University, British Columbia, Canada) and Gideon Davies (University of York, UK). The image, generated with PYMOL (DeLano Scientific LLC, <http://pymol.sourceforge.net/>), shows the observed electron density as a blue “wire-cage” inside the active centre pocket represented by the smooth surface.

Professor Davies was presented with the Roy L Whistler Award of the International Carbohydrate Organization at the XXIIIrd International Carbohydrate Symposium in Whistler in 2006.

© 2007 G. Davies. Published by Elsevier Ltd.

Available online at www.sciencedirect.com



Abstracted/Indexed in: Chem. Abstr.: Curr. Contents: Phys., Chem. & Earth Sci. Life Sci. Current Awareness in Bio. Sci. (CABS). Science Citation Index. Full texts are incorporated in CJELSEVIER, a file in the Chemical Journals Online database which is available on STN[®] International. Also covered in the abstract and citation database SCOPUS[®]. Full text available on ScienceDirect[®]



ELSEVIER

ISSN 0008-6215